nonradiative rate in the case of the glass (see ref 27).

Conclusions

By investigation of the luminescence properties of Ln ions adsorbed onto the pore surface of PVG it is possible to characterize the chemical structure of this system.

The Ln ions occupy a range of sites with somewhat different chemical surroundings. The ions are bound to the silica surface but are also coordinated by water molecules. The number of water molecules coordinating a Ln ion is approximately four. This water coordination is lower than in aqueous solution (nine coordination) due to the fact that the Ln ion is bound to the silica surface on one side and coordinated by water molecules on the other side.

The adsorbed Ln ions can interact with each other. From the observation of energy transfer from Ce^{3+} to Tb^{3+} and from Gd^{3+} to Tb^{3+} it is found that adsorbed Ln ions are on the average separated about 7 Å from each other. The electron-transfer interaction between Ce^{3+} and Eu^{3+} which is known to exist in the solid state is also observed when the ions are adsorbed onto PVG. A maximum quenching distance of about 14 Å is found.

Acknowledgment. We are indebted to R. van Doorn and Z. Vroon for carrying out part of the experimental work.

Registry No. Gd, 7440-54-2; Eu, 7440-53-1; Ce, 7440-45-1; Tb, 7440-27-9; La, 7439-91-0.

(27) Verwey, J. W. M.; Dirksen, G. J.; Blasse, G. *J. Non-Cryst. Solids* **1988**, *107*, 49.

Influence of Annelation on the Electronic Properties of Phthalocyanine Macrocycles

E. Ortí,* M. C. Piqueras, and R. Crespo

Departamento Química Física, Universidad de Valencia, Dr. Moliner, 50, 46100 Burjassot, Valencia, Spain

J. L. Brédas*

Service de Chimie des Matériaux Nouveaux et Département des Matériaux et Procédés, Université de Mons, Avenue Maistriau, 21, B-7000 Mons, Belgium

Received August 8, 1989

We present the results of valence effective Hamiltonian (VEH) nonempirical pseudopotential calculations on the electronic structure of various macrocycles including tetraazaporphyrin, phthalocyanine, 2,3-naphthalocyanine, 1,2-naphthalocyanine, and phenanthrenocyanine. We focus our attention on the evolution of the oxidation potentials and lowest optical absorptions as a function of linear or angular annelation of benzene rings onto the basic tetraazaporphyrin macrocycle. The VEH results are found to agree with cyclic voltammetry and optical absorption experimental data. These results provide a coherent picture of the evolution of the electrical conductivity properties in crystals and polymers derived from those compounds.

Introduction

Phthalocyanine molecular crystals and cofacially linked polymers are well-documented as materials that may attain high electrical conductivities. Environmentally stable compounds with conductivities on the order of 1–1000 S/cm after partial oxidation by iodine have been reported.[1-3] Although most of the synthetic efforts have been devoted to varying the nature of the atom complexed in the cavity (over 70 different phthalocyanine complexes can be obtained by substituting the central two hydrogen atoms by metal or metalloid atoms), investigations of the transport properties[1-3] indicate that the electrical conductivity has very little dependence on the identity of the complexed atom but is strongly influenced by the orientation and spacing of the phthalocyanine rings. Theoretical studies on the electronic band structures of phthalocyanines[4-8] show that a columnar stacking with minimal spacing leads to an optimal interaction between the π-molecular orbitals on adjacent rings and promotes the highest conductivities. More effective π-interactions and hence higher conductivities could thus be expected if the conjugated system of the phthalocyanine macrocycle becomes more extended. Several synthetic efforts have therefore recently been devoted to obtain crystals and polymers derived from tetraazamacrocycles even larger than phthalocyanine.[9-11]

(1) Marks, T. J. *Science* **1985**, *227*, 881.
(2) (a) Hoffman, B. M.; Ibers, J. A. *Acc. Chem. Res.* **1983**, *16*, 15. (b) Palmer, S. M.; Stanton, J. L.; Martinsen, J.; Ogawa, M. Y.; Hener, W. B.; Van Wallendael, S. E.; Hoffman, B. M.; Ibers, J. A. *Mol. Cryst. Liq. Cryst.* **1985**, *125*, 1.
(3) Hanack, M.; Datz, A.; Fay, R.; Fischer, K.; Keppeler, U.; Koch, J.; Metz, J.; Mezger, M.; Schneider, O.; Schulze, H. J. In *Handbook of Conducting Polymers*; Skotheim, T. A., Ed.; Marcel Dekker: New York, 1986; Vol 1, Chapter 5, p 133.
(4) Whangbo, M.-H.; Stewart, K. R. *Isr. J. Chem.* **1983**, *23*, 133.
(5) Canadell, E.; Alvarez, S. *Inorg. Chem.* **1984**, *23*, 573.
(6) Pietro, W. J.; Marks, T. J.; Ratner, M. A. *J. Am. Chem. Soc.* **1985**, *107*, 5387.
(7) Kutzler, F. W.; Ellis, D. E. *J. Chem. Phys.* **1986**, *84*, 1033.
(8) Gómez-Romero, P.; Lee, Y.-S.; Kertesz, M. *Inorg. Chem.* **1988**, *27*, 3672.
(9) Snow, A. W.; Price, T. R. *Synth. Met.* **1984**, *9*, 329.
(10) Hanack, M.; Renz, G.; Strähle, J.; Schmid, S. *Chem. Ber.* **1988**, *121*, 1479.

0897-4756/90/2802-0110$02.50/0

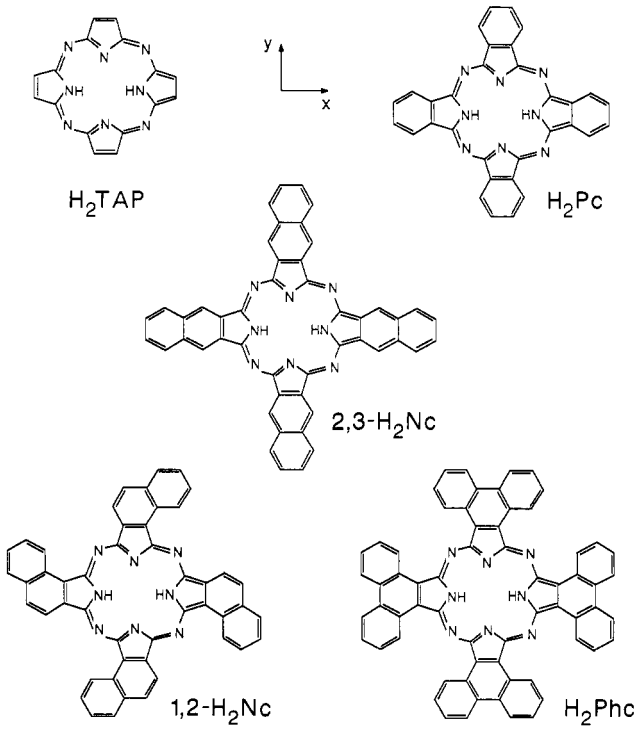

Figure 1. Structures of the metal-free macrocycles investigated in this work: tetraazaporphyrin (H_2TAP), phthalocyanine (H_2Pc), 2,3-naphthalocyanine (2,3-H_2Nc), 1,2-naphthalocyanine (1,2-H_2Nc), and 9,10-phenanthrenocyanine (H_2Phc).

This paper seeks to analyze how the extension of the aromatic structure of the macrocycle affects those molecular electronic properties (ionization potentials, redox potentials, and optical transitions) that are more closely related with electrical conductivity. The extension of the macrocycle structure is carried out by successive annelation of benzene rings. Phthalocyanine itself can be regarded as a derivative of tetraazaporphyrin where the aromatic system has been enlarged by the condensation of four benzene rings. Taking the tetraazaporphyrin molecule as the reference macrocycle to which different polycondensated benzenoid structures are fused, we study the electronic structure of the tetraazamacrocycles presented in Figure 1. These macrocycles correspond to (i) tetraazaporphyrin (H_2TAP), (ii) tetrabenzotetraazaporphyrin, or phthalocyanine (H_2Pc), (iii) tetrakis(2,3-naphtho)tetraazaporphyrin, or 2,3-naphthalocyanine (2,3-H_2Nc), (iv) tetrakis(1,2-naphtho)tetraazaporphyrin or 1,2-naphthalocyanine (1,2-H_2Nc), and (v) tetrakis(9,10-phenanthro)-tetraazaporphyrin or 9,10-phenanthrenocyanine (H_2Phc). Note that 1,2-H_2Nc and H_2Phc can be regarded as derivatives of phthalocyanine with *angular annelation* of the benzene rings, while 2,3-H_2Nc presents a *linear annelation* of the benzene rings.

Experimental Section

The electronic structures of the molecular systems depicted in Figure 1 have been studied by using the valence effective Hamiltonian (VEH) quantum-chemical technique.[12] The VEH method takes into account only the valence electrons and is based on the use of an effective Fock Hamiltonian parametrized to reproduce the results of ab initio calculations. In this way, the VEH method is especially useful in dealing with very large molecular systems since it is completely nonempirical and yields one-electron energies of ab initio double-ζ quality at a reasonable computer cost. All the calculations have been performed using the VEH parameters previously reported for the nitrogen atoms[13] and those recently obtained for the carbon and hydrogen atoms.[14]

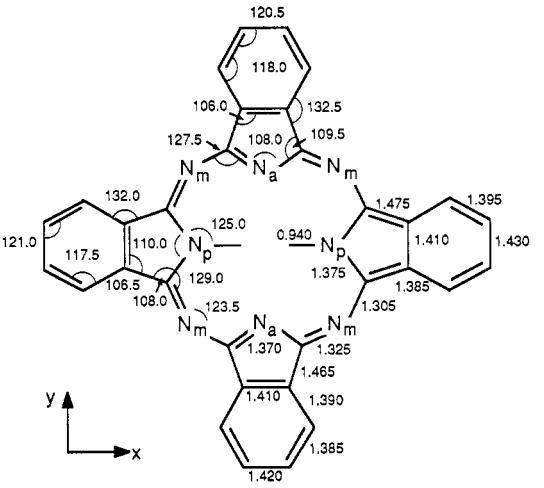

Figure 2. D_{2h} geometry parameters for phthalocyanine. Bond lengths are in angstroms, and bond angles in degrees. N_p denotes a pyrrole nitrogen, and N_a and N_m denote pyrrole aza and meso-bridging aza nitrogens, respectively.

The molecular geometry used for the phthalocyanine molecule is shown in Figure 2, and it is based on the neutron diffraction data reported by Hoskins et al.[15] These authors attribute a planar C_{2h} geometry to the H_2Pc molecule, but a few adjustments have been made to obtain the D_{2h} geometry shown in Figure 2. This geometry has been calculated by taking the arithmetic means of the experimental values for equivalent bonds on opposite isoindole moieties in order to impose symmetry planes passing through the central nitrogens. Although there is some controversy about the location of the two inner hydrogens of metal-free tetraazamacrocycles, these atoms have been placed on opposite nitrogen atoms (see Figure 2) in accordance with the experimental data for phthalocyanine[16] and the closely related porphine and tetraphenylporphine molecules.[17,18] It is to be noted that VEH calculations were both performed on the reported C_{2h} geometry[15] and the averaged D_{2h} structure. Since both geometries lead to identical results, only the results based on the D_{2h} symmetry are presented here.

The geometry displayed in Figure 2 has been used to build up the central tetraazaporphyrin ring in the tetraazaporphyrin, 2,3-naphthalocyanine, and phenanthrenocyanine molecules, which do not have any structural data. The input geometries for 2,3-naphthalocyanine and phenanthrenocyanine have been obtained by fusing the experimental structures reported for naphthalene[19] and phenanthrene[20] to the tetraazaporphyrin ring. The atomic coordinates used for 1,2-naphthalocyanine have been taken from the X-ray diffraction data on its doubly substituted iron derivative 1,2-$NcFe(RCN)_2$, and they define a C_{2h} geometry.[10]

To discuss the optical properties of the macrocycles investigated in this work, two features should be considered in relation to the theoretical approach:

(11) Hanack, M.; Lange, A.; Rein, M.; Behnisch, R.; Renz, G.; Leverenz, A. *Synth. Met.* **1989**, *29*, F1.
(12) (a) Nicolas, G.; Durand, Ph. *J. Chem. Phys.* **1979**, *70*, 2020; (b) *Ibid.* **1980**, *72*, 473. (c) Andrê, J. M.; Burke, L. A.; Delhalle, J.; Nicolas, G.; Durand, Ph. *Int. J. Quantum Chem. Symp.* **1979**, *13*, 283. (d) Brêdas, J. L.; Chance, R. R.; Silbey, R.; Nicolas, G.; Durand, Ph. *J. Chem. Phys.* **1981**, *75*, 255.
(13) Brêdas, J. L.; Thêmans, B.; Andrê, J. M. *J. Chem. Phys.* **1983**, *78*, 6137.
(14) Thêmans, B.; Andrê, J. M.; Brêdas, J. L. To be published.
(15) Hoskins, B. F.; Mason, S. A.; White, J. C. B. *J. Chem. Soc., Chem. Commun.* **1969**, 554.
(16) (a) Niwa, Y.; Kobayashi, H.; Tsuchida, T. *J. Chem. Phys.* **1974**, *60*, 799; (b) *Inorg. Chem.* **1974**, *13*, 2891.
(17) (a) Silvers, S. J.; Tulinsky, A. *J. Am. Chem. Soc.* **1967**, *89*, 3331. (b) Chen, B. M. L.; Tulinsky, A. *Ibid.* **1972**, *94*, 4144.
(18) (a) Wehrle, B.; Limbach, H.-H.; Köcher, M.; Ermer, O.; Vogel, E. *Angew. Chem., Int. Ed. Engl.* **1987**, *26*, 934. (b) Frydman, L.; Olivieri, A. C.; Diaz, L. E.; Frydman, B.; Morin, F. G.; Mayne, C. L.; Grant, D. M.; Adler, A. D. *J. Am. Chem. Soc.* **1988**, *110*, 336.
(19) Bastiansen, O.; Skancke, P. N. *Adv. Chem. Phys.* **1961**, *3*, 323.
(20) Kao, J. *J. Am. Chem. Soc.* **1987**, *109*, 3817.

Table I. VEH One-Electron Energy Levels ($-\epsilon_i$, in electronvolts) Obtained for Tetraazaporphyrin (H_2TAP), Phthalocyanine (H_2PC), 2,3-Naphthalocyanine (2,3-H_2NC), 1,2-Naphthalocyanine (1,2-H_2Nc), and 9,10-Phenanthrenocyanine (H_2Phc)[a]

H_2TAP[b]		H_2Pc[b]		2,3-H_2Nc[b]		1,2-H_2Nc[b]		H_2Phc[b]	
$3a_u^*$	4.43	$5a_u^*$	3.85	$10b_{1u}^*$	4.30	$16a_u^*$	4.35	$9a_u^*$	4.58
$4b_{3g}^*$	5.56	$6b_{3g}^*$	4.93	$8b_{2g}^*$	4.88	$16b_g^*$	5.22	$10b_{2g}^*$	5.44
$4b_{2g}^*$	5.74	$6b_{2g}^*$	5.10	$8b_{3g}^*$	4.88	$15b_g^*$	5.36	$10b_{3g}^*$	5.44
$2a_u$	7.27	$4a_u$	6.32	$6a_u$	5.93	$15a_u$	6.60	$8a_u$	6.75
$5b_{1u}$	9.75	$7b_{1u}$	9.32	$5a_u$	8.50	$14a_u$	8.57	$11b_{1u}$	8.39
$4b_{1u}$	9.76	$5b_{2g}$	9.36	$7b_{2g}$	8.59	14_{bg}	8.60	$10b_{1u}$	8.45
$3b_{3g}$	9.79	$6b_{1u}$	9.36	$7b_{3g}$	8.59	$13a_u$	8.64	$9b_{2g}$	8.45
$3b_{2g}$	9.80	$5b_{3g}$	9.37	$4a_u$	8.90	$13b_g$	8.65	$9b_{3g}$	8.45
$3b_{1u}$	10.61	$3a_u$	9.66	$9b_{1u}$	9.24	$12a_u$	9.29	$7a_u$	8.75

[a] The highest six occupied and the lowest three unoccupied levels are included. All orbitals are of π-nature. [b] Energy values before introducing any adjustments to calculate the energy of electronic transitions (see text for further details).

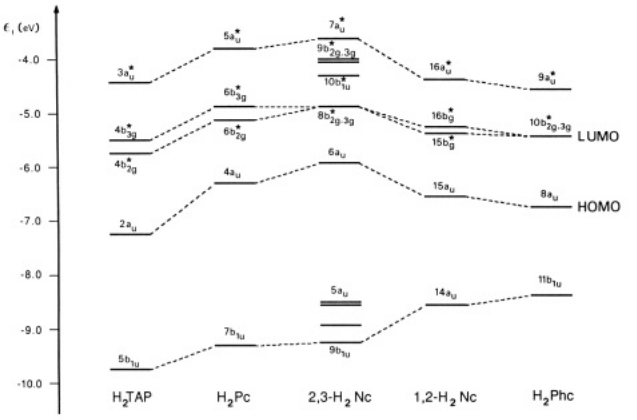

Figure 3. Calculated VEH one-electron energies (ϵ_i) and symmetries of the upper occupied and lower unoccupied molecular orbitals. All the orbitals are of π-type.

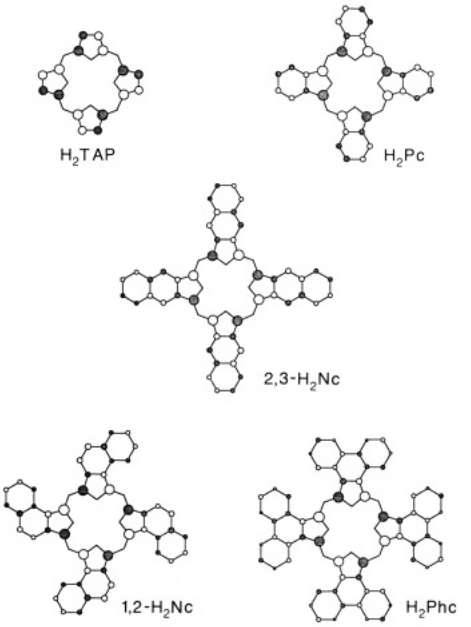

Figure 4. Atomic orbital (AO) composition of the a_u highest occupied molecular orbitals. The size of the circles is approximately proportional to the magnitude of the AO coefficients. A white area indicates a positive value for the upper lobe of the p_zAO, while a grey area indicates a negative value.

(i) The VEH method yields, as in any other ab initio technique, also wide valence electronic structures, and a contraction of the energy scale for the occupied valence levels becomes necessary to obtain the best correlation with experimental photoemission data. A contraction factor of 1.3 has been consistently used as discussed in Ref 21.

(ii) The VEH method predicts a HOMO–LUMO energy gap of only 1.22 eV for the phthalocyanine molecule, underestimating the energy of the first optical transition (1.81 eV) reported from vapor absorption spectra for H_2Pc by 0.59 eV.[22]

Therefore, the energies of electron transitions from the occupied to the unoccupied levels are calculated as one-electron energy differences after contracting the energy scale for the occupied levels by a factor of 1.3 and rigidly shifting the unoccupied levels by 0.59 eV to higher energies. It must be stressed that identical adjustments have been successfully employed earlier in the case of various phthalocyanine compounds.[23] These adjustments are systematically used in *all* the molecular systems investigated in this work in order to provide a consistent approach and meaningful comparisons.

Results and Discussion

The VEH one-electron energy level distributions obtained for the five molecular systems shown in Figure 1 are collected in Table I and schematically displayed in Figure 3. Only the highest occupied and lowest unoccupied molecular orbitals are included in Figure 3 because they determine the most interesting electronic properties. All these orbitals are of π-nature, the first occupied σ-orbitals lying below −10.3 eV. They have been classified according to the D_{2h} point group of symmetry except for the 1,2-naphthalocyanine molecule, which assumes a C_{2h} geometrical structure. Molecular orbitals in Figure 3 have been correlated on the basis of their atomic orbital composition.

Table I and Figure 3 indicate that the highest occupied molecular orbital (HOMO) corresponds, in all cases, to a level of a_u symmetry. It is important to note that this level shows the same atomic orbital patterns for all the systems studied here. As shown in Figure 4, the a_u HOMOs are spread over the carbon backbone *with no contribution from the nitrogen atoms*. This feature has been previously discussed for the phthalocyanine molecule.[21]

An energy destabilization of the HOMO level is observed in Figure 3 when comparing tetraazaporphyrin and phthalocyanine. The $4a_u$ HOMO of phthalocyanine is located at −6.32 eV, in agreement with the first ionization energy (6.41 eV) obtained from the gas-phase UPS spectrum of H_2Pc.[24] For tetraazaporphyrin, the $2a_u$ HOMO is calculated to lie at −7.27 eV, which is about 1 eV below the HOMO of phthalocyanine. Photoemission data are not available in the literature for tetraazaporphyrin; however, the VEH one-electron energy obtained for the tetraazaporphyrin HOMO correlates very well with the first ion-

(21) Ortí, E.; Brédas, J. L. *J. Chem. Phys.* **1988**, *89*, 1009.
(22) Edwards, L.; Gouterman, M. *J. Mol. Spectrosc.* **1970**, *33*, 292.
(23) Ortí, E.; Brédas, J. L.; Clarisse, C. *J. Chem. Phys.*, in press.
(24) Berkowitz, J. *J. Chem. Phys.* **1979**, *70*, 2819.

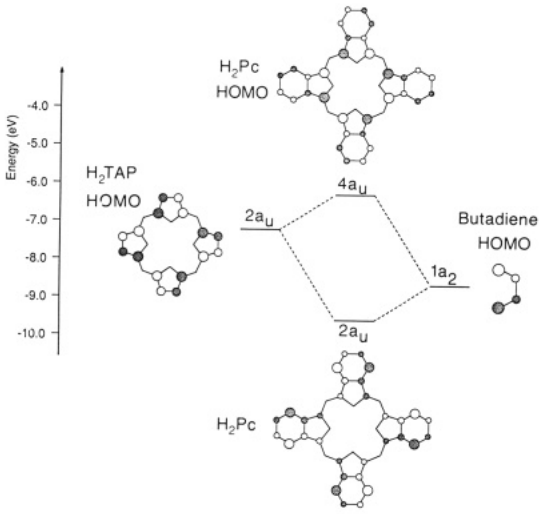

Figure 5. Molecular orbital diagram for the interaction between the HOMO of tetrazaporphyrin and the HOMO of *cis*-butadiene fragments leading to phthalocyanine.

ization energy (6.9–7.1 eV) experimentally reported for the metal-free porphine molecule (H_2P).[25] Since the only difference between tetraazaporphyrin and porphine resides in the four aza nitrogen (N_m in Figure 2) atoms linking the pyrrole units (these nitrogen atoms do not contribute to the HOMO level), similar ionization potentials should be expected for both molecules. Indeed, preliminary VEH calculations predict almost equal energies for the HOMO levels of H_2TAP and H_2P (−7.27 vs −7.39 eV, respectively).[26]

The destabilization of the HOMO level from tetraazaporphyrin to phthalocyanine can be understood in terms of the interaction diagram shown in Figure 5. Here, the $2a_u$ HOMO of H_2TAP located at −7.27 eV interacts with the stabler $1a_2$ HOMO of four butadiene fragments at an energy of −8.85 eV. The antibonding interaction between these orbitals destabilizes the $2a_u$ HOMO of tetraazaporphyrin and gives rise to the $4a_u$ HOMO of phthalocyanine, while the bonding interaction produces the $2a_u$ molecular orbital of H_2Pc embedded in a group of orbitals below −9.32 eV (see Table I). Similar arguments can be used to interpret the additional destabilization of the HOMO level observed in Table I and Figure 3 when four butadiene fragments interact with the phthalocyanine moiety to produce the 2,3-naphthalocyanine molecule. The $6a_u$ HOMO level is located at −5.93 eV (0.39 eV above the $4a_u$ HOMO of phthalocyanine).

Since oxidation involves removing an electron from the HOMO, it is reasonable to expect that molecules with lower lying HOMOs have larger oxidation potentials. In this way, the relative stabilities of the HOMO levels predicted by the VEH method justify the larger oxidation potentials measured for phthalocyanine compounds which are compared to those observed for 2,3-naphthalocyanine compounds.[11] For example, a redox potential of 1.15 V is reported for the oxidation of the phthalocyanine macrocycle in cobalt phthalocyanine compared to a value of 0.77 V obtained for the oxidation of the naphthalocyanine macrocycle in cobalt 2,3-naphthalocyanine. Both potentials were recorded by cyclic voltammetry in pyridine/Bu_4NClO_4 by using a saturated calomel reference electrode (SCE).[11] Similarly, oxidation potentials of 1.00 and 0.58 V vs SCE have been measured in CH_2Cl_2 for $SiPc(OR)_2$ and $SiNc(OR)_2$ compounds, respectively.[27] The differences between these oxidation potentials (0.38 V for the cobalt compounds and 0.42 V for the silicon compounds) correlate very well with the VEH energy difference (0.39 eV) that separates the HOMOs of H_2Pc and 2,3-H_2Nc. Although no oxidation potential is available for the tetraazaporphyrin system, a similar decrease of the oxidation potentials is observed in going from the closely related porphyrin (1.2–1.4 V)[28] to the more extended tetrabenzotetraazaporphyrin (phthalocyanine) systems (0.7–1.1 V).[29] This trend agrees with the destabilization of the HOMO level calculated for phthalocyanine with respect to tetraazaporphyrin.

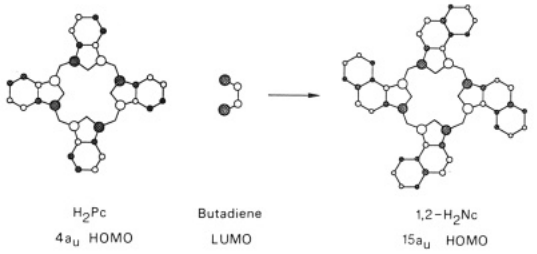

Figure 6. Bonding interaction between the HOMO of phthalocyanine and the LUMO of *cis*-butadiene fragments leading to 1,2-naphthalocyanine.

In contrast to 2,3-H_2Nc, the condensation of benzene rings in an angular fashion to obtain 1,2-naphthalocyanine and phenanthrenocyanine gives rise to a slight stabilization of the HOMO levels; these levels are located at −6.60 (1,2-H_2Nc) and −6.75 eV (H_2Phc) with respect to phthalocyanine (−6.32 eV). This stabilization is the result of the weak bonding interaction that takes place between the $4a_u$ HOMO of H_2Pc and the $2b_1$* LUMO of the butadiene fragments located at −3.95 eV, as is shown in Figure 6 in the case of 1,2-naphthalocyanine. For both 1,2-naphthalocyanine and phenanthrenocyanine, the perturbation of the $4a_u$ HOMO of phthalocyanine by the $1a_2$ HOMO of butadiene would lead to a nonbonding interaction. Experimental redox data on 1,2-naphthalocyanine compounds are scarce and, to the best of our knowledge, have been reported only in the case of the iron derivative; the oxidation potential of 1,2-FeNc (1.01 V) is measured to be very similar to that reported for FePc (1.10 V).[11]

The VEH results indicate that the extension of the conjugated system by annelation of benzene rings following the axis of the pyrrole units (*linear annelation*) produces a continuous destabilization of the highest occupied molecular orbital and, consequently, a decrease in the oxidation potential of the macrocycle. On the contrary, *angular annelation* of benzene rings, as in 1,2-H_2Nc and H_2Phc, slightly stabilizes the HOMO level with respect to H_2Pc, and similar oxidation potentials can be expected. These trends agree with the evolution experimentally observed in polycondensated benzenoid hydrocarbons, for which the first ionization potential undergoes a continuous decrease when linear annelation is performed but is quite insensitive to angular annelation.[30] Furthermore, these trends help in rationalizing the electrical conductivity values reported for 2,3-FeNc (4×10^{-5} S/cm) and the

(25) Dupuis, P.; Roberge, R.; Sandorfy, C. *Chem. Phys. Lett.* **1980**, *75*, 434.
(26) Ortí, E.; Brédas, J. L. In *Chemical Physics of Intercalation*; Legrand, A. P., Flandrois, S., Eds.; Plenum Press: New York, 1987; p 501.
(27) Wheeler, B. L.; Nagasubramanian, G.; Bard, A. J.; Schechtman, L. A.; Dininny, D. R.; Kenney, M. E. *J. Am. Chem. Soc.* **1984**, *106*, 7404.
(28) Fuhrhop, J. H.; Kadish, K. M.; Davis, D. G. *J. Am. Chem. Soc.* **1973**, *95*, 5140.
(29) Wolberg, A.; Manassen, J. *J. Am. Chem. Soc.* **1970**, *92*, 2982.
(30) (a) Clar, E.; Schmidt, W. *Tetrahedron* **1975**, *31*, 2263; (b) *Ibid.* **1979**, *35*, 2673.

Table II. VEH Electronic Transitions Calculated for Tetraazaporphyrin and Phthalocyanine[a]

transition	energy[b]	oscillator strength	polarization[c]
	H_2TAP		
$2a_u \rightarrow 4b_{2g}^*$	2.12 (586)	4.5	y
$2a_u \rightarrow 4b_{3g}^*$	2.30 (539)	3.9	x
$5b_{1u} \rightarrow 4b_{2g}^*$	4.03 (308)	0.8	x
$4b_{1u} \rightarrow 4b_{2g}^*$	4.04 (307)	1.4	x
$5b_{1u} \rightarrow 4b_{3g}^*$	4.21 (294)	0.5	y
$4b_{1u} \rightarrow 4b_{3g}^*$	4.22 (294)	1.5	y
	H_2Pc		
$4a_u \rightarrow 6b_{2g}^*$	1.81 (685)	5.1	y
$4a_u \rightarrow 6b_{3g}^*$	1.98 (625)	4.7	x
$4a_u \rightarrow 7b_{2g}^*$	3.90 (318)	0.4	y
$4a_u \rightarrow 7b_{3g}^*$	3.91 (317)	0.3	x
$7b_{1u} \rightarrow 6b_{2g}^*$	4.12 (301)	1.6	x
$6b_{1u} \rightarrow 6b_{2g}^*$	4.15 (299)	0.3	x
$7b_{1u} \rightarrow 6b_{3g}^*$	4.29 (289)	1.6	y
$6b_{1u} \rightarrow 6b_{3g}^*$	4.32 (287)	0.3	y

[a] Transitions more energetic than 4.3 eV or with oscillator strengths lower than 0.1 are not included. Energies are in electronvolts (nanometers in parentheses). [b] Transition energies are calculated as one-electron energy differences after a contraction of 1.3 of the occupied levels and a shift of 0.59 eV to higher energies of the unoccupied levels. See text for details. [c] Axes refer to those presented in Figure 1.

corresponding 1,4-diisocyanobenzene-bridged (dib) polymer $[2,3\text{-NcFe(dib)}]_n$ (2×10^{-3} S/cm) obtained without any intentional *external* doping.[31] The high conductivity of these compounds compared to that of FePc (2.5×10^{-10} S/cm)[32] and $[\text{PcFe(dib)}]_n$ (2×10^{-5} S/cm)[33] is actually caused by oxygen doping from the air, which becomes possible due to the low oxidation potential of the naphthalocyanine ring. This feature is important since it leads to environmentally stable doped systems with electrical conductivities that are sufficiently high for a good deal of applications. In contrast, the conductivities reported for the 1,2-FeNc (4×10^{-9} S/cm) and $[1,2\text{-NcFe(dib)}]_n$ (6×10^{-10} S/cm) compounds[10] and FePhc (8×10^{-9} S/cm) and $[\text{PhcFe(dib)}]_n$ (4×10^{-12} S/cm) compounds[34] are very similar to those of the phthalocyanine compounds.

We now discuss the possible molecular orbital interpretation of the optical absorption spectra displayed by the macrocycles investigated in this work. The optical spectra of square-planar porphyrins and related macrocyclic systems are mainly characterized by an intense electronic absorption band in the visible region (Q band) and another broad absorption band in the near-ultraviolet region (B or Soret band). The VEH energies and oscillator strengths calculated for the electronic transitions corresponding to these bands are presented in Tables II and III. As discussed above, these energies represent one-electron differences obtained from the ground-state levels (Figure 3) after a contraction of 1.3 of the energy scale for the occupied levels and a rigid shift of 0.59 eV to higher energies for the unoccupied levels.

The lowest unoccupied molecular orbital (LUMO) corresponds to b_{2g} or b_{3g} π^*-molecular orbitals (see Table I and Figure 3), which have nonzero coefficients on the pyrrole or the aza nitrogens (N_p and N_a in Figure 2), respectively. The near degeneracy of these two orbitals (which are separated by about 0.15 eV in tetraazaporphyrin, phthalocyanine, and 1,2-naphthalocyanine) is due to the almost identical geometry of the carbon–nitrogen backbone along the x and y axes (see Figures 1 and 2). This degeneracy is more pronounced for 2,3-naphthalocyanine and phenanthrenocyanine since no geometrical structure is available for these systems. We have also assumed that identical aromatic units are fused to the tetraazaporphyrin rings along the x and y axes. Thus, almost no energy difference is calculated between the b_{2g} and b_{3g} levels in 2,3-naphthalocyanine and phenanthrenocyanine (see Table I). These features imply that the carbon–nitrogen π-electron system essentially corresponds to an effective D_{4h} symmetry.

Table III. VEH Electronic Transitions Calculated for 2,3-Naphthalocyanine, 1,2-Naphthalocyanine, and Phenanthrenocyanine[a]

transition[b]	energy[c]	oscillator strength	polarization[d]
	$2,3\text{-}H_2Nc$		
$6a_u \rightarrow 8b_{3g}^*, 8b_{2g}^*$	1.64 (757)	5.2	x, y
$6a_u \rightarrow 9b_{3g}^*, 9b_{2g}^*$	2.50 (496)	1.7	x, y
$5a_u \rightarrow 8b_{3g}^*, 8b_{2g}^*$	3.62 (343)	1.4	x, y
$4a_u \rightarrow 8b_{3g}^*, 8b_{2g}^*$	3.93 (315)	1.1	x, y
$9b_{1u} \rightarrow 8b_{3g}^*, 8b_{2g}^*$	4.19 (296)	2.0	x, y
$8b_{1u} \rightarrow 8b_{3g}^*, 8b_{2g}^*$	4.21 (294)	0.6	x, y
	$1,2\text{-}H_2Nc$		
$15a_u \rightarrow 15b_g^*$	1.84 (675)	4.8 (1.5)[e]	x, y
$15a_u \rightarrow 16b_g^*$	1.97 (629)	1.5 (4.6)	x, y
$14a_u \rightarrow 15b_g^*$	3.35 (371)	0.8 (1.6)	x, y
$13a_u \rightarrow 15b_g^*$	3.40 (365)	0.1 (1.5)	x, y
$14a_u \rightarrow 16b_g^*$	3.48 (356)	1.4 (0.6)	x, y
$13a_u \rightarrow 16b_g^*$	3.54 (351)	0.8 (0.5)	x, y
$12a_u \rightarrow 15b_g^*$	3.90 (318)	1.4 (0.1)	x, y
$15a_u \rightarrow 18b_g^*$	3.96 (313)	0.3 (0.1)	x, y
$12a_u \rightarrow 16b_g^*$	4.04 (307)	0.2 (1.3)	x, y
$11a_u \rightarrow 15b_g^*$	4.07 (304)	0.5 (1.1)	x, y
	H_2Phc		
$8a_u \rightarrow 10b_{3g}^*, 10b_{2g}^*$	1.88 (661)	4.9	x, y
$11b_{1u} \rightarrow 10b_{3g}^*, 10b_{2g}^*$	3.14 (395)	2.2	x, y
$10b_{1u} \rightarrow 10b_{3g}^*, 10b_{2g}^*$	3.18 (390)	0.7	x, y
$7a_u \rightarrow 10b_{3g}^*, 10b_{2g}^*$	3.41 (364)	0.9	x, y
$6a_u \rightarrow 10b_{3g}^*, 10b_{2g}^*$	3.45 (359)	0.6	x, y
$8a_u \rightarrow 11b_{2g}^*, 11b_{3g}^*$	3.73 (332)	0.5	x, y
$9b_{3g}, 9b_{2g} \rightarrow 9a_u^*$	4.07 (304)	1.1	x, y
$5a_u \rightarrow 10b_{3g}^*, 10b_{2g}^*$	4.14 (299)	1.1	x, y

[a] Transitions more energetic than 4.2 eV or with oscillator strengths lower than 0.1 are not included. Energies in electronvolts (nanometers in parentheses). [b] The way the geometries of $1,2\text{-}H_2Nc$ and H_2Ph are built (see text for details) determines the degeneracy of the b_{2g}^*–b_{3g}^* molecular orbitals since almost no structural difference exists between aromatic moieties along the x and y axes (see Figure 1). [c] Transition energies are calculated as one-electron energy differences after a contraction of 1.3 of the occupied levels and a shift of 0.59 eV to higher energies of the unoccupied levels. See text for details. [d] Axes refer to those presented in Figure 1. [e] Numbers in parentheses refer to oscillator strengths along the y axis.

The theoretical data in Tables II and III indicate that very intense electronic transitions (oscillator strengths of about 5) are obtained in the visible region for all the molecular systems studied in this work. These transitions correspond to the promotion of an electron from the a_u HOMO levels to the b_{2g}^*–b_{3g}^* LUMOs and can be clearly correlated with the Q absorption band observed experimentally. For tetraazaporphyrin, the $2a_u \rightarrow 4b_{2g}^*$ and $2a_u \rightarrow 4b_{3g}^*$ electronic transitions have energy values of 2.12 (586 nm) and 2.30 eV (539 nm), respectively. These values agree with the sharp absorption peaks at 2.01 (617 nm, Q_x band) and 2.27 eV (545 nm, Q_y band) recorded for tetraazaporphyrin in chlorobenzene solution.[35] Taking into account that the VEH calculations for tetraazaporphyrin

(31) Deger, S.; Hanack, M. *Synth. Met.* **1986**, *13*, 319.
(32) Day, P.; Soregg, G.; Williams, R. J. P. *Nature* **1963**, *197*, 589.
(33) Schneider, O.; Hanack, M. *Chem. Ber.* **1983**, *116*, 2088.
(34) Renz, G. Ph.D. Thesis, University of Tübingen, 1989.
(35) Linstead, R. P.; Whalley, M. *J. Chem. Soc.* **1952**, 4839.

have been performed on a model geometry as discussed above, both the splitting of the Q band (0.26 eV) and the relative intensity of the constituent peaks (Q_x more intense than Q_y) are very well reproduced by the theoretical calculations. By general convention, the lowest energy Q band is referred to as Q_x without implying any absolute orientation. The important fact is that when adopting x axis as the axis defined by the central two hydrogens, the lowest energy Q_x band is calculated to be polarized following the y axis (see Table II), i.e., perpendicular to the H–H axis.

As can be seen from Table II, a bathochromic shift of the long-wavelength transitions is observed in going from tetraazaporphyrin to phthalocyanine. In the latter case, the $4a_u \rightarrow 6b_{2g}^*$ and $4a_u \rightarrow 6b_{3g}^*$ electronic transitions appear at 1.81 (685 nm) and 1.98 eV (625 nm), respectively. This bathochromic shift is a result of the narrowing of the HOMO–LUMO energy gap in phthalocyanine compared with that calculated for tetraazaporphyrin (see Figure 3). This shift agrees with the longer wavelength transitions experimentally observed for phthalocyanine. The Q_x and Q_y bands for phthalocyanine vapors are measured at 686 and 623 nm, respectively.[22]

The condensation of additional benzene rings leads to different results, depending on the way the rings are fused. Linear annelation to obtain 2,3-naphthalocyanine produces an additional narrowing of the HOMO–LUMO energy gap (see Figure 3) and a bathochromic shift of the lowest energy optical transition (see Table III). This transtion ($6a_u \rightarrow 8b_{3g}^*$, $8b_{2g}^*$) is now located at 1.64 eV (757 nm) and agrees with the absorption Q_x band measured at 750 nm for a derivative of 2,3-FeNc in chloroform.[11] The single-peak structure of the theoretical transition contrasts with the double absorption experimentally observed and is due to the geometry used for 2,3-H_2Nc in the VEH calculations. This geometry removes the small splitting actually present between the $8b_{3g}^*$ and $8b_{2g}^*$ levels.

In contrast to 2,3-naphthalocyanine, angular annelation to obtain 1,2-naphthalocyanine and phenanthrenocyanine produces no significant effect on the HOMO–LUMO energy gap. These molecules retain the main absorption characteristics of phthalocyanine. The lowest energy electronic transitions are calculated to occur at energy values of 1.84 (675 nm) and 1.88 eV (661 nm) for 1,2-H_2Nc ($15a_u \rightarrow 15b_g^*$) and H_2Phc ($8a_u \rightarrow 10b_{3g}^*$, $10b_{2g}^*$). These values are almost equal to those calculated for H_2Pc (1.81 eV), and they agree with those experimentally reported for octahedrally complexed iron derivatives of 1,2-H_2Nc (653 nm) and H_2Phc (657 nm) in chloroform.[11] Note that the same derivative of H_2Pc presents the first absorption peak at 658 nm.[11]

For all the molecular systems studied in this work except 2,3-naphthalocyanine, the next relevant theoretical transition involves the excitation of an electron from the second HOMO to the LUMO (see Tables II and III). In the case of phthalocyanine, this transition corresponds to the $7b_{1u} \rightarrow 6b_{2g}^*$ excitation and is calculated at an energy of 4.12 eV. However, this transition is embedded in a group of very close-lying transitions starting with the $4a_u \rightarrow 7b_{2g}^*$ excitation at 3.90 eV. This group of theoretical transitions can be correlated with the broad B or Soret band measured to be centered at 3.65 eV and to extend from 3.3 to 4.1 eV.[22] For tetraazaporphyrin, a group of four transitions ($4b_{1u}$, $5b_{1u} \rightarrow 4b_{2g}^*$, $4b_{3g}^*$) is computed to lie around 4.10 eV, i.e., at almost the same energy as that obtained for H_2Pc (4.12 eV). This result agrees with the almost equal energies reported for the B bands of tetrazaporphyrin (3.72 eV)[35] and phthalocyanine (3.65 eV).[22] Similar transitions appear for 1,2-naphthalocyanine ($13a_u$, $14a_u \rightarrow 15b_g^*$, $16b_g^*$) and phenanthrenocyanine ($6a_u$, $7a_u$, $10b_{1u}$, $11b_{1u} \rightarrow 10b_{3g}^*$, $10b_{2g}^*$), but they are now located at about 3.45 and 3.30 eV, respectively. This shift to longer wavelengths agrees with the bathochromic shift of the B band observed for 1,2-FeNc (3.50 eV) and FePhc (3.42 eV) compounds compared to FePc compounds (3.80 eV).[11,34]

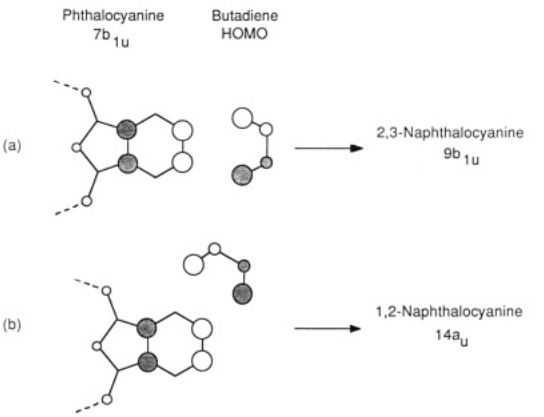

Figure 7. Antibonding interaction between the b_{1u} molecular orbital of H_2Pc and the HOMO of *cis*-butadiene fragments leading to (a) 2,3-naphthalocyanine and (b) 1,2-naphthalocyanine.

As can be seen from Figure 3, 2,3-naphthalocyanine presents an energy level distribution pattern different from the other macrocycles. Here, a group of four molecular orbitals appears above the $9b_{1u}$ level, which has the same atomic orbital composition as the $7b_{1u}$ level of H_2Pc, and another group of four molecular orbitals appears below the $7a_u^*$ level, which correlates with the $5a_u^*$ level of H_2Pc. As a result (see Table III), a new transition at an energy of 2.50 eV (496 nm) is calculated for 2,3-naphthalocyanine due to the promotion of an electron from the $6a_u$ HOMO to the low-lying $9b_{3g}^*$, $9b_{2g}^*$ levels. The appearance of this transition can be correlated with the complication of the spectral pattern in the region of the B band for zinc 2,3-tetranaphthoporphyrin (Zn-2,3-TNP) compared with zinc tetrabenzoporphyrin (Zn-TBP).[36] We note that the B band lies around 400–450 nm for Zn-TBP,[36,37] i.e., the same wavelength region where the new transition appears. Electronic transitions from the second $5a_u$ HOMO to the $8b_{3g}^*$ and $8b_{2g}^*$ LUMO's occur at similar energies (3.62 eV) as in 1,2-H_2Nc and H_2Phc. Finally, the electronic transition $9b_{1u} \rightarrow 8b_{3g}^*$, $8b_{2g}^*$, which clearly corresponds to the $7b_{1u} \rightarrow 6b_{2g}^*$, $6b_{3g}^*$ transition of H_2Pc (4.12 eV) associated to the B absorption band, appears at 4.19 eV.

The VEH results thus predict that linear annelation produces a red shift of the first absorption band Q while the second absorption band B remains mainly unaffected. In contrast, angular annelation induces almost no change for band Q but shifts band B to longer wavelengths. As discussed earlier, the evolution observed for the Q band is mostly due to the energetic behavior of the HOMO level. Similarly, the evolution obtained for the B band can be rationalized as the result of the interaction between the second HOMO of the macrocycle and the HOMO of butadiene fragments. This interaction is shown in Figure 7 for the phthalocyanine macrocycle. If the *cis*-butadiene fragments are added in a linear fashion to give 2,3-naphthalocyanine (Figure 7a), no effective interaction between the fragments and the macrocycle is possible due to the local symmetries. However, if butadiene fragments

(36) Kuz'mitskii, V. A.; Solov'ev, K. N.; Knyukshto, V. N.; Shushkevich, I. K.; Kopranenkov, V. N.; Vorotnikov, A. N. *Russ. Org. Teor. Eksp. Khim.* **1983**, *19*, 655.
(37) Edwards, L.; Gouterman, M.; Rose, C. B. *J. Am. Chem. Soc.* **1976**, *98*, 7638.

are added on the side to produce 1,2-naphthalocyanine (Figure 7b), a strong antibonding interaction takes place. As a result, the b_{1u} occupied level remains almost unaffected when passing from phthalocyanine to 2,3-naphthalocyanine, but it is strongly destabilized upon formation of 1,2-naphthalocyanine or phenanthrenocyanine (see Figure 3). The trends obtained for the Q and B bands agree with those observed for both linearly and angularly annelated polycondensated benzenoid hydrocarbons.[30]

Compared to standard ab initio Hartree–Fock calculations, the VEH method provides good estimates for the lowest energy optical transitions. As previously discussed,[13] this feature is due to the fact that the VEH parametrization is not contaminated by any information coming from the unoccupied Hartree–Fock molecular orbitals. However, it must be borne in mind that we are working in a single-configuration approach and an important configuration interaction is to be expected when electronic transitions of the same symmetry take place at similar energies. This configuration mixing can be important for states leading to the B absorption band, and no clear theoretical assignment of this band is possible, as described elsewhere.[23] It can therefore be concluded that the four-orbital model, originally developed by Weiss et al.[38] to justify the absorption features of free-base porphine, is not valid to explain the origin of band B in tetraazaporphyrin compounds since several electronic transitions are involved in this band. The complex nature of band B is supported by magnetic circular dichroism spectra reported for phthalocyanine.[39] These spectra suggest that there are at least three distinct types of excitations in region B involving π-molecular orbitals.

Conclusions

The theoretical results obtained here show that for phthalocyanine-type macrocycles, linear annelation leads to a more effective conjugation in the macrocyclic system than does angular annelation, which agrees with the general trends reported for polyacene series by Clar and Schmidt.[30] The main effects of annelation on the electronic properties of tetraazamacrocycles are summarized as follows:

(i) Linear annelation produces a continuous destabilization of the HOMO level. As a result, a decrease of the first ionization potential and a narrowing of the HOMO–LUMO energy gap are both observed in going from tetraazaporphyrin to phthalocyanine and from phthalocyanine to 2,3-naphthalocyanine. Therefore, a continuous decrease of the oxidation potential of the macrocycle and a bathochromic shift of the lowest energy electronic transition (Q band) are predicted along the series H_2TAP, H_2Pc, 2,3-H_2Nc. On the other hand, linear annelation leaves the second highest occupied molecular orbital mostly unaffected, and similar energies are obtained for the electronic transitions involved in the region of the B absorption band. It is to be noted that 2,3-naphthalocyanine presents more complicated spectral features in this energy region due to the appearance of additional transitions at intermediate energies.

(ii) Angular annelation affects the HOMO level to a lesser extent, and similar oxidation potentials and transition energies in the visible region are expected for 1,2-naphthalocyanine and phenanthrenocyanine, as compared with phthalocyanine. In contrast, angular annelation induces a significant destabilization of the b_{1u} second highest occupied orbital, and a continuous bathochromic shift of the near ultraviolet B band is predicted along the series H_2Pc, 1,2-H_2Nc, H_2Phc.

These results agree with the cyclic voltammetry and optical absorption experimental data and thus allow us to fully rationalize the general trends observed for these tetraazamacrocycles.

In conclusion, the VEH results indicate that due to the lower oxidation potentials and narrower energy gaps, better conductivity properties are to be expected for crystals and polymers derived from linearly annelated than from angularly annelated phthalocyanine macrocycles. This prediction is consistent with the higher electrical conductivities reported for 2,3-naphthalocyanine compounds, and it leads to the possibility of obtaining environmentally stable oxygen-doped systems with sufficiently high conductivities for a number of applications. Furthermore, preliminary VEH calculations on more extended linearly annelated phthalocyanines suggest the possibility of obtaining crystals and polymers with very small bandgaps, for example, a HOMO–LUMO energy gap of only 1.07 eV is predicted when fusing tetracene units to the tetraazaporphyrin macrocycle. Further work along these lines is in progress.

Acknowledgment. We thank the CIUV (Centro de Informática de la Universidad de Valencia) for the use of their computing facilities. R.C. is grateful to the Ministerio de Educación y Ciencia for a Doctoral grant. E.O. is indebted to the University of Mons for its hospitality and financial support and also to the Generalitat Valenciana for a grant. This work has been partly supported by Project No. 683.2/89 from the University of Valencia and the DGICYT Project PS88-0112. Finally, we are indebted to Professor M. Hanack for communicating unpublished data.

Registry No. H_2TAP, 500-77-6; H_2Pc, 574-93-6; 2,3-H_2Nc, 23627-89-6; 1,2-H_2Nc, 10094-23-2; H_2Phc, 124441-38-9.

(38) Weiss, C.; Kobayashi, H.; Gouterman, M. *J. Mol. Spectrosc.* **1965**, *16*, 415.
(39) Martin, K. A.; Stillman, M. J. *Can. J. Chem.* **1979**, *57*, 1111.